2004

Magnetic Susceptibility for the Paleocene-Eocene Boundary: Correlation among Three Egyptian Sections

Kelli Willson

Magnetic Susceptibility for the Paleocene-Eocene Boundary: Correlation among Three Egyptian Sections

by

Kelli Willson

Submitted as an Honors Thesis

to

Louisiana State University, Department of Geology and Geophysics, E235 Howe-Russell Geosciences Complex, Baton Rouge, LA 70808

TITLE PAGE

TABLE OF CONTENTS

Magnetic Susceptibility for the Paleocene – Eocene Boundary: Correlation among Three Egyptian Sections

Kelli Willson

Honors Thesis, Louisiana State University, Department of Geology and Geophysics

ABSTRACT

With the recent selection of the Dababiya DBH section in upper Egypt as the Global Boundary Stratotype Section and Point (GSSP) for the Paleocene – Eocene (P-E) boundary, now based on a negative carbon isotope ($\delta^{13}C$) excursion (CIE), other research is possible into alternate means for global correlation and interpretation of P-E boundary sections. A technique that has been used for this purpose is magnetic susceptibility (MS). MS provides an easy, quick, and inexpensive method for correlation and paleoclimatic interpretation, which is also independent of gross lithology. A total of 776 samples were collected from three Paleocene-Eocene boundary interval sections in Egypt and the magnetic susceptibility (MS) measured and correlated to the biostratigraphic and $\delta^{13}C$ data sets chosen to represent the beginning of the Eocene at the GSSP. Each section displayed a distinctive MS signature at the boundary showing a rapid increase and MS pulses above the CIE. These increases are associated with the Paleocene Eocene Thermal Maximum (PETM) which occurred immediately following the CIE and is reported by others (Röhl et al., 2000). The PETM represents a time of

significant global warming and the MS variations reflect the variable erosion and detrital influx of sediment into the marine environment during this time of oscillating warm-wet climate.

INTRODUCTION

The Paleocene – Eocene boundary marks the division between the Thanetian and Ypresian geological stages and is dated at approximately 55 Ma. During this period of Earth's history, there was a massive sudden input of ~1,200 to 2,000 gigatons of carbon (as methane) into the atmosphere, causing a geologically significant global warming (Norris et al., 1999). The methane release could have been caused by the decomposition of sedimentary methane gas hydrates on the ocean floor or through other processes. The residence time of carbon in the atmosphere is ~120,000 years, and it has been argued this input of carbon resulted in a long term alteration of global climate (Norris et al., 1999). This change in environment produced evolutionary pressure that produced new species and caused the extinction of others, phenomena evident in the fossil record at and above the boundary. For example, the earliest horse species, *Hyracotherium,* evolved at this time; while approximately 30-50% of all benthic foraminiferal taxa went extinct (Röhl et al., 2000). There was a near total reversal of global ocean water current flow over a period of less than 100,000 years (Norris et al., 1999). This occurred as warm, dense, saline water moved from Tethyan marginal areas outward to fill oceanic basins. The wide dissemination of warm ocean surface waters allowed for tropical climate expansion into high

latitudes. Over a period of ~50,000 years, the carbon isotopic ratio changed from pre-event levels to full excursion levels (2 to 0 $\delta^{13}C$), a trend that supports the hypothesis of gas hydrate release in the oceans (Röhl et al., 2000). This period of global warming and widespread tropical climate is referred to as the Paleocene – Eocene Thermal Maximum (PETM).

The present-day area of the Nile Valley in Egypt (Fig. 1) provides an excellent record of the PETM environment in the southern Tethyan seaway. The precise location of the Paleocene-Eocene boundary is known at the Dababiya Quarry Sections, as this is where the P-E boundary is gloabally defined based on the CIE. The CIE also identifies the boundary at Wadi Nukhul and Jebel Qreiya. However, more means of correlation are needed in order to locate the boundary in sections that are lacking the CIE. This project is intended to show MS utility for correlating the P-E boundary using sections in which this boundary is already identified. Once this is established, MS can be used as an alternate or supplemental method of correlation in other sections worldwide. Even though the CIE is the globally defining event that marks the P-E boundary, other methods are needed in order to locate the boundary within sections lacking the CIE.

Paleocene-Eocene Thermal Maximum (PETM)

At the P-E boundary, there was an abrupt shift in the global climate pattern that is identifiable through geochemical methods. This period represents a reorganization of global carbon cycling and ocean circulation patterns that created rapid and severe global warming. The PETM is characterized by a global, reduction of the latitudinal temperature gradient caused by a warming of

the deep oceans. This warming caused a depletion of oxygen near the seafloor, killing off many species of benthic foraminifera. The PETM resulted from several massive, sudden inputs of carbon into the atmosphere through the apparent release of gas hydrates in the seafloor.

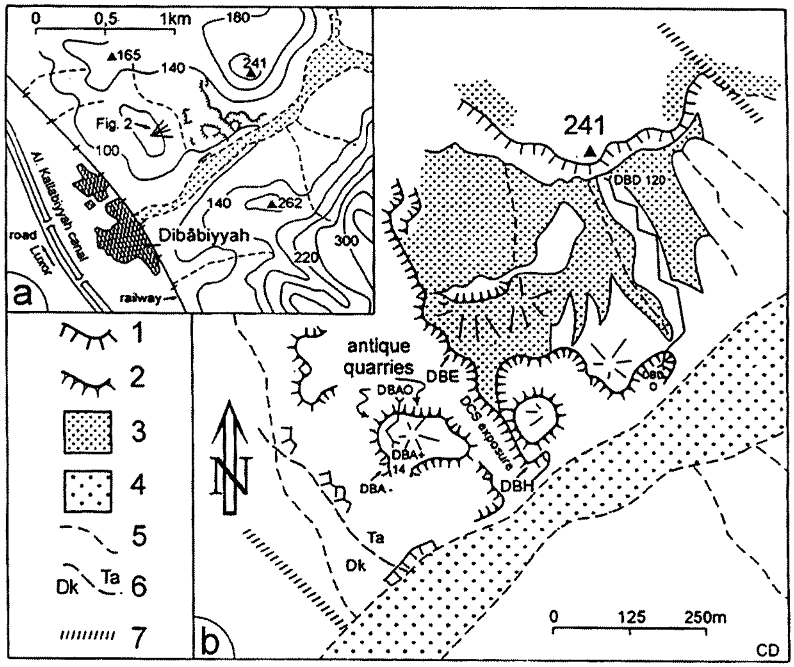

Fig. 1 – Map view of Dababiya study area taken from (Dupuis et al., 2003). a: Dababiya study area and relative position of Luxor-Aswan Road; b: detailed map showing the Dababiya Quarries and position of DBH GSSP section; legend: 1, natural cliffs; 2, quarry fronts; 3, screes; 4, wadi (dry river bed); 5, thalweg; 6, Dahkla/ Tarawan contact; 7, faults.

It is estimated that these pulsed events lasted ~1000 years (Röhl et al., 2000). Each of these events was followed by a hiatus ~20 k.y. in length (Röhl et al., 2000), during which little carbon isotopic change took place. The input/hiatus

cycles lasted ~80 k.y., at which time $\delta^{13}C$ values returned to pre-excursion levels (Röhl et al., 2000).

Several lines of geochemical evidence support the PETM patterns seen in the rock record, including $\delta^{13}C$, $\delta^{18}O$, and $CaCO_3$ and iron content. Sedimentation rates were estimated using cycle thickness tied to Milankovich precessional band timing. There is a three-fold decrease in sedimentation rate immediately preceding the PETM across Egypt. Sedimentation rate then increased and leveled off during the 50 k.y. following the PETM (Röhl et al., 2000). The hiatus periods during which no carbon pulses occurred may have been caused by a temporary halt in methane hydrate release, or to the balance between release of carbon and the preferential burial of ^{12}C in reservoirs. Röhl et al. (2000) estimate that the entire PETM lasted ~220 k.y., but that pre-event levels of $\delta^{13}C$ were achieved within ~50 k.y.

Paleocene-Eocene Boundary Sections

The Global Boundary Stratotype Section and Point (GSSP) for the Paleocene-Eocene Boundary

The Dababiya Quarry section in Upper Egypt (Fig. 1) was chosen as the GSSP and formally adopted in early 2004. It is located in an inactive quarry on the east bank of the Nile River and east of the Luxor-Aswan Road. The quarry is approximately 1 km east of the village of Dababiya and ~35 km south of Luxor. The section represents an open marine setting, possibly ranging from neritic to upper bathyal (Ouda, 2003). The entire section imcludes the Dakhla Shale,

Tarawan Chalk, Esna Shale, and the Thebes Limestone over ~130 m (Fig. 2). All beds dip gently eastward.

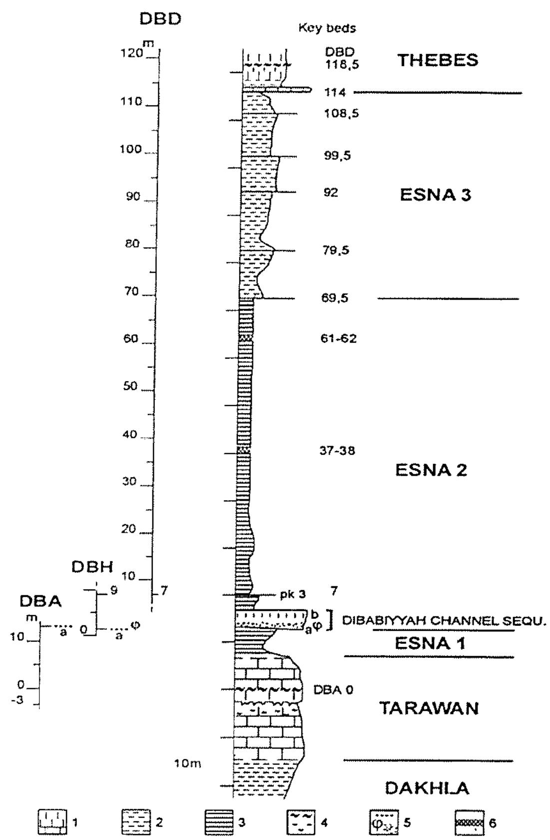

Fig. 2 – Lithology of Dababiya sections DBA, DBH (GSSP section), and DBD. legend: 1, limestone; 2, marls and shales; 3, shales; 4, flint concretions; 5, phosphates; 6, variegated shales (from Dupuis et al., 2003).

This section was selected as the GSSP due to the near complete biostratigraphic, chemostratigraphic, and lithologic records across the boundary. Ten meters of the top of the greenish calcareous shale of the Dakhla Formation is exposed at the base of the section (Fig. 3), with the white unbedded Tarawan Chalk, above, measuring ~20 m in thickness. The Tarawan transitions into a

stratified, greenish, bioturbated shale near the base of a unit of the Esna shale, Esna Unit 1 is ~7 m thick at Dababiya and is overlain by Esna Unit 2. Within the Esna 1-Esna 2 P-E boundary interval is the Dababiya Channel Sequence (DCS; Fig. 2) composed of thin clay beds beneath a phosphatic coprolite-rich shale grading into thick fossiliferous calcareous mudstone. The DCS grades into Esna 2 that is generally lithologically homogeneous being clayey, dark in color, and unbedded. The DCS at Dababiya, ~3.7 m thick, is characterized by basal dark grey clay marking the P-E boundary (Fig. 4), phosphatic and calcareous shale, and finally calcarenitic limestone. Esna Unit 3 consists of alternating layers of marls and limestone beds, which are lighter in color than the underlying Esna 2. The base of the Thebes limestone is taken to be the base of the thickest limestone package in the section because the upper Esna 3 possesses some smaller transitional limestone beds within it.

The geochemistry of the Dababiya Quarry section contains a negative CIE seen in other sections around the world and therefore this CIE has been chosen as the P-E boundary marker event. The $\delta^{13}C$ excursion of -3‰ is located in the base of the DCS and also correlates with the most massive extinction of benthic foraminifera in the last 90 million years. This is termed the Benthic Foraminifera Extinction (BFE). The P-E boundary was traditionally defined based on the Highest Occurrence of *Morozovella velascoensis*. Above this level, $\delta^{13}C$ values show a gradual increase and return to normal pre-excursion carbon isotopic levels (Dupuis, 2003). Therefore, the totality of the event and recovery is recorded in the DCS beds at Dababiya. Biostratigraphic work has shown that the

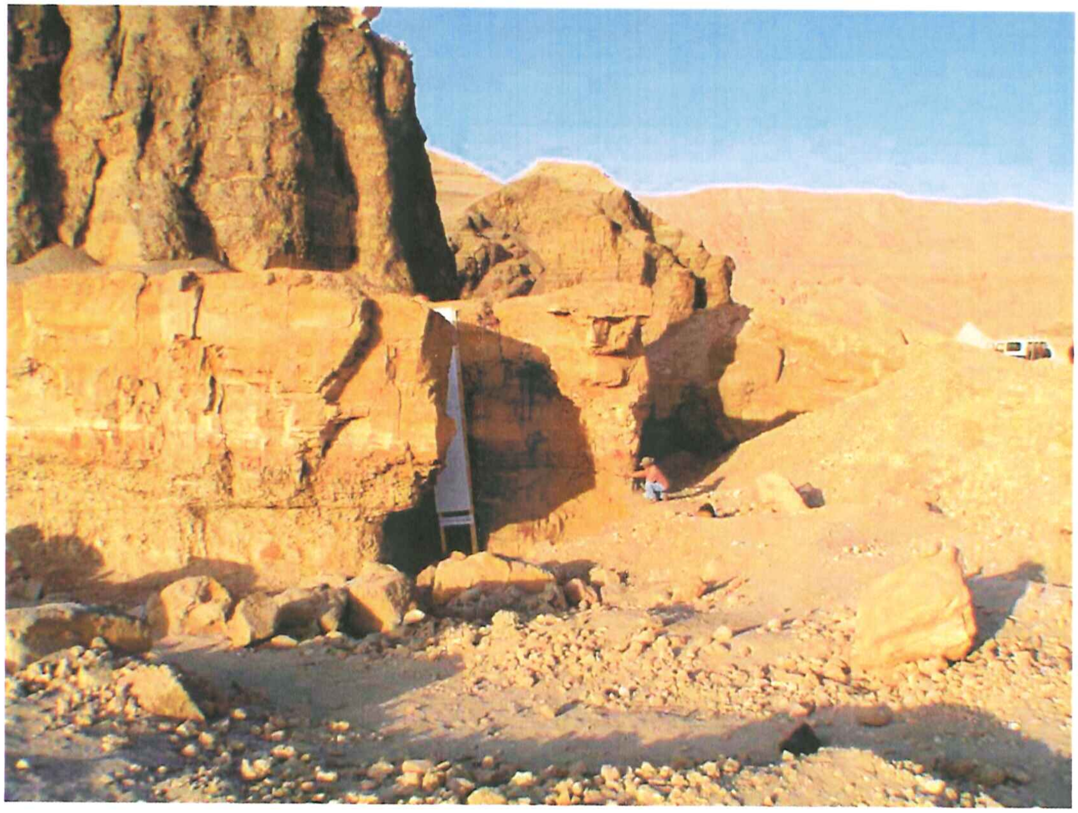

Fig. 3 - View of GSSP section, Dababiya Quarry, Upper Egypt. The boundary layer is indicated by the figure's arm. Photo courtesy of Brooks Ellwood.

organic carbon shift seen in this GSSP section corresponds to the CIE seen in all other P-E sections in Egypt that have been studied.

Preservation of microfossils in this section ranges from excellent to poor, depending on the lithology. Even so, the microfossil record is sufficiently complete to show extinctions below and repopulations of new species above the boundary. Typical planktonic foraminiferal assemblages for the top of Esna 1 within the DB Quarry include *Morozovella velascoensis, M. acuta, M. aequa, M. subbotinae,* and *Acarinina soldadoensis* (Dupuis, 2003). The DCS is bracketed below by the Last Occurrence of *A. esnanensis, Igorina broedermanni, A. angulosa,* and *A. wilcoxensis* and above by the LO of *Pseudohastigerina*

wilcoxensis (Berggren, 2003). The calcareous nannofossil assemblage directly above the boundary layer includes the newly evolved species *Rhomboaster* spp., *Pontosphaera* spp., *Discoaster anartios*, and *D. araneus* (Dupuis, 2003). Many of these microfossils are excursion taxa that develop and go to extinction all within the CIE interval. The benthic foraminiferal assemblage, consisting of newly evolved species *Anomalinoides aegyptiacus* and *A. zitteli* originating in the CIE interval's benthic foraminifera extinction, suggests an outer neritic environment with a depth of 150-175 m (Dupuis, 2003).

Fig. 4 - DCS in outcrop at GSSP section, Dababiya Quarry, Upper Egypt. Photo courtesy of Brooks Ellwood.

Jebel Qreiya

The Jebel Qreiya section of the central Nile Valley provides a near complete stratigraphic sequence from the Upper Cretaceous to lower Eocene. Located at the southern end of Jebel Abu Had in Upper Egypt, it is ~50 km northeast of the town of Qena and ~110 km NNE of the GSSP in the DB Quarry. J. Qreiya is located to the east of the Nile River, off the Qena-Safaga Road in the Eastern Desert: Latitude 26° 21'N and Longitude 33° 01' E. The beds dip gently eastward.

The J. Qreiya section contains the same lithologies represented in the DB Quarry (Fig. 2). Oldest strata are within the Dakhla Formation which here is composed of yellow marls and greenish grey shales. This sequence includes the uninterrupted Cretaceous – Tertiary boundary, but it is lacking the distinctive boundary clay layer (Ouda, 2003). Overlying the Dakhla Formation is the Tarawan Formation, here composed of ~9 m of white unbedded chalky limestone grading into pale greenish grey poorly fissile mudstone. Lying immediately above the Tarawan is the Esna Formation, which is here subdivided into three members, covering ~46 m. Esna 1, the oldest member, overlies the Tarawan Chalk and is ~7.4 m of homogenous mudstone with sparse delicate burrows at Jebel Qreiya. At the Esna 1/ Esna 2 boundary is found the DCS sedimentary package (Fig. 2), but here the DCS is approximately 2.5 m thick. The DCS grades into Esna 2, a monotonous, poorly fissile olive-grey mudstone. Here there is an unconformable base to the overlying Esna 3, which is a paler, more calcareous mudstone with thin limestone interbeds. Finally, the Thebes

Formation overlies the Esna Formation, consisting of thick unbedded limestone with some chert nodules at the base. Here, the Thebes Formation is approximately 140 m thick. The J. Qreiya section is lithologically similar to the other P-E sections described in Egypt, the difference being that the J. Qreiya section lacks an unconformity between the Tarawan Chalk and Esna 1.

The geochemistry reported for J. Qreiya supports evidence for global warming, with a negative CIE at the P-E boundary. Here the CIE is -3‰, within the range of normal CIE values for other Egyptian P-E sites (Knox et al, 2003). The CIE pattern of a rapid fall followed by a gradual increase in carbon isotopic values is seen in all P-E sites, including J. Qreiya. Again, this supports the argument for a sudden input of large quantities of methane gas into the atmosphere, which would cause the large carbon isotope excursion seen in these sections (Norris et al, 1999). At the J. Qreiya section, a peak in the percentage of kaolinite within the sediments coincides with the CIE level (Soliman, 2003). The shale within the P-E boundary layer contains the largest abundance of kaolinite at the CIE level, followed by a decline in kaolinite above the CIE. Such increases in kaolinite indicate a warm, wet climate at the CIE level or erosion of kaolinite-rich sediments. There is also a higher proportion of chlorite and illite coincident with the CIE, which suggests an increased supply of clays.

The contact between the Tarawan Chalk and Esna 1 in the J. Qreiya section is defined based on the Lowest Occurence of planktonic foraminifera *Acarinina soldadoensis* and *Morozovella aequa*, and the Highest Common Occurrence of *Igorina albeari* and *Acarinina subsphaerica* (Knox et al., 2003).

The upper part of the CIE at J. Qreiya, as at the Dababiya quarry, is marked by changes in the abundance of planktonic foraminifera and the complete extinction of most benthic foraminifera. However, the calcareous nannoplankton and benthic foraminiferal zonal boundaries are indistinct and disputed. This is due to poor calcareous nannoplankton preservation in the Esna shale beds. A distinct succession of benthic foraminiferal assemblages was recognized at J. Qreiya: *Angulogavelinella avnimelechi* below the CIE, *Anomalinoides aegyptiacus* in the lower portion of the CIE, and *Bulimina callahani* in the upper portion of the CIE (Dupuis, 2003).

Wadi Nukhul

A west central Sinai P-E section was collected at Wadi Nukhul, located on the northeast side of the Gulf of Suez. The lithology is similar to the GSSP (Fig. 2) and J. Qreiya sections, with the Tarawan Chalk, Esna Shale, and Thebes Limestone in outcrop. The Benthic Formainifera Extinction and CIE lie within the Dababiya Channel Sequence. The CIE interval spans ~1 m at the base of the DCS, with $\delta^{13}C$ excursions to -3‰ (Ouda, 2003). The Tarawan Chalk is ~2 m thick, much thinner at Wadi Nukhul than at J. Qreiya, while the Esna Shale is ~22 m thick and spans the biostratigraphic foraminiferal zones P4 to P6b of BKSA95 and calcareous nannofossil zones NP9 to NP11 (Ouda, 2003), although these zonations are also contested due to poor preservation of compressed and partially dissolved fossils. The biostratigraphic data are thus limited and inconclusive. The Lowest Occurence of *T. bramlettei* followed by the Highest Occurence of *M. velascoensis* are found above the CIE at Wadi Nukhul (Ouda, 2003).

MAGNETIC METHODS

In preparation for sampling, each of the three sections reported here was first cleaned by scraping and brushing to expose fresh surfaces representing continuous exposure. Samples from each of the sections were then collected and returned to LSU for magnetic susceptibility (MS) measurements. The GSSP section at Dababiya (Fig. 1) was collected in intervals of 5 cm over 3.8m, with spacing reduced to 2 cm within the DCS interval, and covered the Esna 1, Esna 2, and DCS boundary interval, for a total of 90 samples. The sample interval for Jebel Qreiya was 10 cm measured through 55 m of section for a total of 550 samples. This sampling scheme encompassed the Dakhla Formation up to the Esna 2-Esna 3 contact. The Wadi Nukhul section was sampled at intervals ranging from 5 to 10 cm over 12 m, for a total of 136 samples. Sampling at Wadi Nukhul began in the Tarawan Chalk and ended in the Esna Shale, ~3-4 m above the DCS boundary interval.

The MS was measured in the rock magnetism laboratory at LSU by placing each sample in an A.F. magnetic induction bridge. Induced magnetism was measured three times for each sample. An average of the three values was used in calculating the MS relative to sample mass, and reported in m^3/kg.

MS has several advantages associated with its use as a correlation tool, including ease, low expense, and rapid measurement (Ellwood, 2001). Sample size can be very small, to ~1 gm of sample, and samples do not need to be oriented for measurement. While magnetic polarity studies require stable

ferrimagnetic minerals to acquire a measureable remanent magnetization, MS in marine sediments originates from a combination of all compounds in a sample. It has been shown that detrital and eolian paramagnetic minerals, including clays, are responsible for the MS signal. Ferromagnesian and other minerals combined with a small ferrimagnetic-component, all fairly stable during diagenesis, also have some affect on the MS (Ellwood, 2000). Diamagnetic minerals, including calcite, feldspar, and quartz, are minerals that exhibit negative induced magnetization, so they generally do not significantly contribute to the MS. This is because the signal from paramagnetic constituents is much greater than from diamagnetic minerals. Thus, a relatively small amount of a paramagnetic material can produce the dominant signal, even if there is an abundant diamagnetic constituent (Ellwood, 2001). In addition, MS is relatively unaffected by low to moderate heating, unlike remanent magnetism samples which can be remagnetized.

MAGNETIC RESULTS

All three sections that were sampled and measured produced similar MS patterns which allow correlation among the P-E boundary sections across Egypt. The GSSP section at Dababiya (Figure 5), shows the characteristic MS event pattern and recovery interval corresponding to the PETM. The Esna 1 shale displays an overall gradual increase and then decrease in MS up the section. There is a decrease in MS immediately below the Esna 1/Esna 2 contact which marks the P-E boundary. Within the boundary clay, there is a sharp increase in

MS, which then decreases just above the boundary within the phosphatic coprolite rich shale. The MS recovery zone corresponds to the interval following a mass extinction event identified in the section. This interval at Dababiya covers 1.2m.

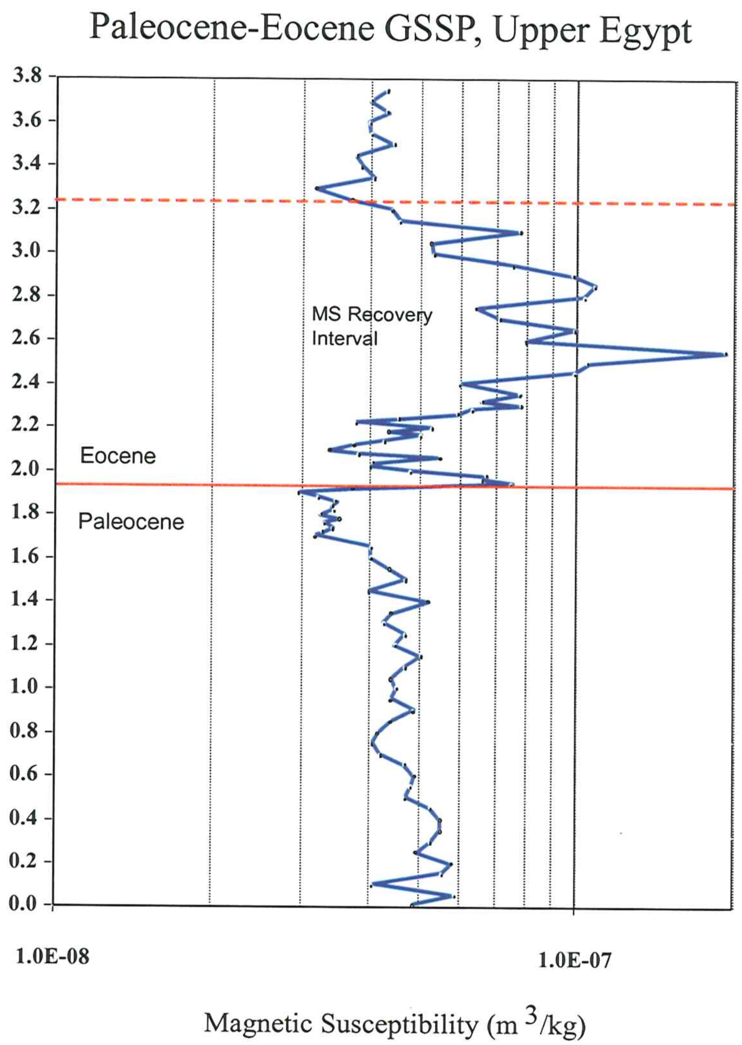

Fig. 5 – MS signal of P-E boundary from the Dababiya GSSP. P-E boundary is characterized by a sharp rise in MS, marked with a solid red line. MS recovery interval is shown, ending at the dashed red line. Note the DCS boundary interval was collected with a 2 cm sample spacing.

The Jebel Qreiya section yielded the broadest picture of the regional MS of Egypt for the Paleocene. There is a sharp increase in MS at the Tarawan/Esna 1 boundary, and the Tarawan Chalk in general has a lower MS than the overlying

Esna 1 shale (Figure 6). The Esna 1 shale above the Tarawan Chalk may exhibit small scale cyclicity and a gradual increase to ~47.5 m in the section.

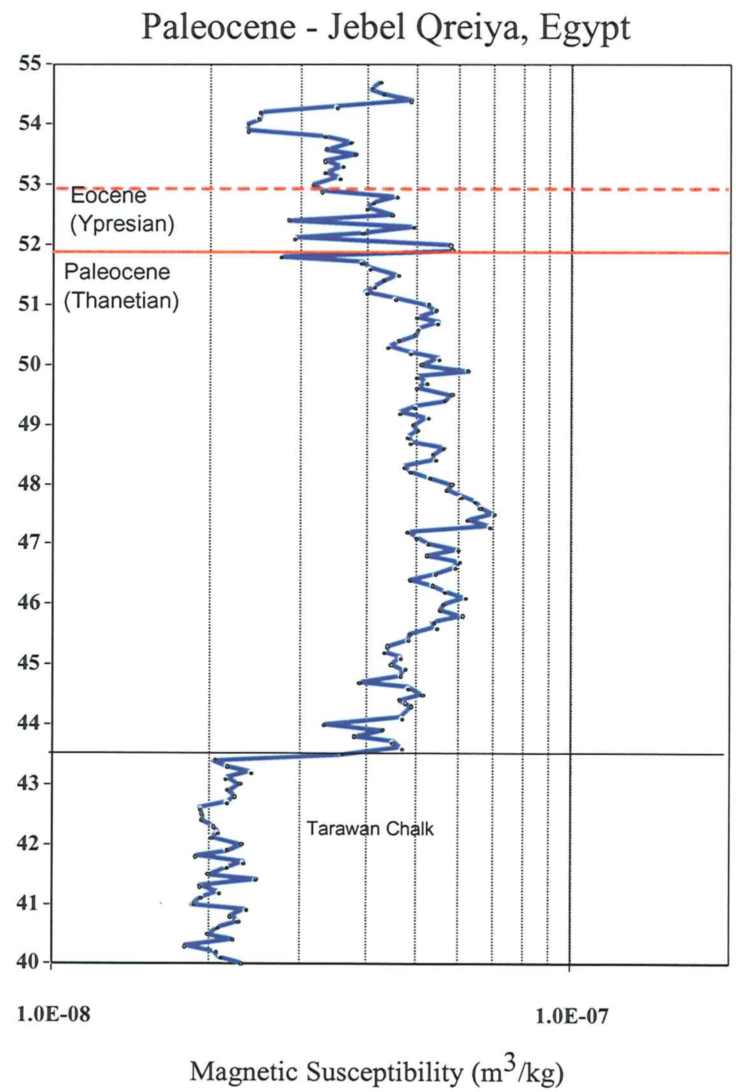

Fig. 6 – MS signal from Jebel Qreiya section. Note the Tarawan has a lower MS than the overlying Esna Shale. P-E boundary is marked with a solid red line. The end of the MS recovery interval is delineated with a dashed red line. Note the J. Qreiya section DCS boundary interval was collected with a 10 cm sample spacing, there it is not as well defined as is the MS for the GSSP.

Above this height the MS trend flattens and then falls to a level immediately below the Esna 1/Esna 2 contact (P-E boundary level). This decrease in MS leads

directly into a jump in MS at the boundary, followed by relatively large swings in MS through approximately 1m of section. Above the MS recovery interval (dashed line in Fig. 6), the MS settles to a moderate MS values through the rest of the sampled interval.

The Wadi Nukhul section displays a similar pattern of MS rise and fall below the boundary interval and a corresponding MS recovery interval. At the base of the measured section, the Tarawan Chalk shows low MS values (Fig. 7), with an abrupt rise in MS at the Tarawan/Esna 1 boundary, seen in the J. Qreiya MS values. The Esna 1 shale shows general MS cyclicity up to the Esna 2 contact. At the P-E boundary level, MS rises and then sharply falls directly above the boundary. The low values mark the beginning of the MS recovery interval for the Wadi Nukhul section. The Wadi Nukhul recovery interval continues up through the remainder of the sampled section, approximately 5 m, and is much thicker here than in the two Upper Egypt sections.

DISCUSSION

Each of the Egyptian sections studied shows the same major trends at and immediately above the boundary. The sharp increase in susceptibility across the boundary, followed by a sharp decrease above the boundary, is present in each section and reflected in their MS signals. This dramatic increase in MS results from rapid erosion and deposition of clays and other detrital and/or eolian components into the marine system. Because detrital and eolian material contains paramagnetic and ferrimagnetic compounds, increased erosion rates will increase MS. These results are interpreted to be in response to the warmer and wetter

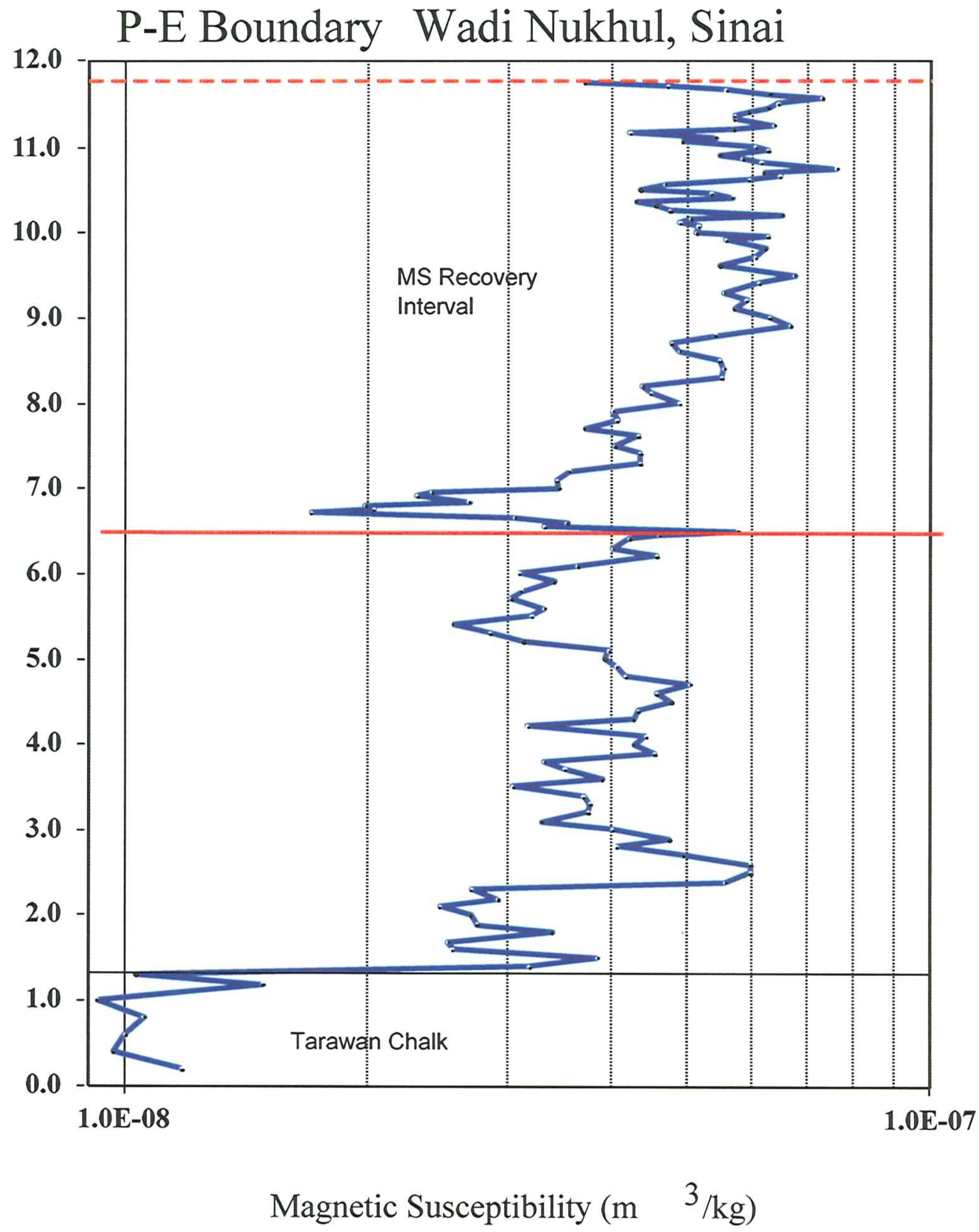

Fig. 7 – MS signal showing P-E boundary from Wadi Nukhul section. Boundary indicated by solid red line and is typified by a sharp increase in MS. Dashed red line shows end of the MS recovery interval, which is characterized by large scale fluctuations in MS and is much thicker than at the GSSp or at J. Qreiya in upper Egypt, indicating a higher sedimentation rate for the Wadi Nukhul section.

climates of the PETM causing a rise in MS values due to increased erosion during wet times.

The variation in pattern seen in each MS recovery interval reflects the global warming driven cycles suggested by others (Röhl et al., 2000). The MS signal above the CIE boundary event is dominated in each section by large scale fluctuations. These are interpreted as proxies for the global processes dealing with the restoration of pre-event conditions, and mirror the δ^{13} C pulses argued to have produced the PETM (Röhl et al., 2000). Because these trends can be ties to global climate, it is expected that the general MS trends observed in Egypt will be correlatable on a worldwide scale. For example, the P-E iron signature from ODB hole 690 in the high latitude south Atlantic shows the same general trends (Röhl et al., 2000) as the MS in these Egyptian sections.

Magnetic Susceptibility was used in this project in order to show its utility as another means of relative dating. Ease of measurement and low cost are several of the advantages associated with MS use as a correlation tool. When comparing the different MS curves, it is important that the sample interval and sedimentation rates be carefully evaluated. The sample interval at Dababiya in the DCS boundary interval was 2.0 cm/sample and the sampled boundary and MS recovery interval was only ~1.2 m thick. The Jebel Qreiya section was uniformly collected at 10 cm intervals over 55 m. The DCS P-E boundary and recovery interval at J. Qreiya is approximately 1 m, similar to the DB GSSP. This means that while at the DB GSSP, the DCS boundary interval and recovery zone is represented in ~60 samples, the equivalent interval at J. Qreiya is only represented

by ~10 samples. Therefore, the character of the DCS boundary interval at J. Qreiya is only poorly defined relative to the DB GSSP. Definition is somewhat better for the Wadi Nukhul section, where the DCS boundary and MS recovery interval is much thicker (~5 m), indicating a sedimentation rate ~5 times that at the DB GSSP and J. Qreiya sections. Therefore, even though sample interval is less than at the DB GSSP, MS resolution at Wadi Nukhul is still high. The higher resolution of the DB GSSP and Wadi Nukhul section allows for a better interpretation of the MS signal through these sections. The large sample interval at the Jebel Qreiya section resulted in less MS signal resolution within the recovery interval making interpretation more difficult. While the Tarawan Chalk was not recovered in samples from the GSSP, this unit was recovered from both the J. Qreiya and Wadi Nukhul sections, where it shows distinctively lower values. The lower values are interpreted to represent a transgressive event that occurred shortly before the end of the Paleocene, during which time deposition switched from shale to chalk.

CONCLUSIONS

The integration of magnetic susceptibility (MS) data sets from three Egyptian sections allows for excellent correlation among these Paleocene – Eocene boundary interval sections. Dababiya GSSP, Jebel Qreiya, and Wadi Nukhul, tied to biostratigraphy and isotope stratigraphy all show the same distinct event boundary pattern reflected in the MS signals. The pattern of low to high MS across the boundary followed by another decrease in MS above the boundary

level and cyclicity pulses within a corresponding recovery pattern interval is consistent among all three sections. It is expected that these correlations will be reflected in other much more distant P-E sections. Independent of gross lithology, easy, quick, and inexpensive, MS may help to identify events in sections that would be otherwise difficult to study. Even though all three sections had different sedimentation rates, environments, and geographic locations, MS was able to define the specific boundary event in each section and tie them all together. Used in connection with other lines of evidence, such as biostratigraphic extinctions, δ^{13} C pulses and lithostratigraphy, it is clear that MS can be an effective climate proxy that aids definition of the P-E boundary. These and the MS variations observed are consistent with erosional pulses associated with global warming during the Paleocene-Eocene Thermal Maximum.

ACKNOWLEDGEMENTS

The author would like to thank Dr. Brooks Ellwood for his help during this project. His continued support and instruction have proved invaluable to my education. I would also like to thank Dr. Steve Benoist for his assistance and encouragement throughout my college career. Logistical support was provided by Dr.'s Aziz Kafafy and Ahmed Kassab of Egypt, and their help is gratefully acknowledged. Samples were collected by Dr.'s Ellwood, Kafafy and Kassab, and Sue Ellwood. This work was funded by a Joint Egypt-US Cooperative grant to Dr.'s Ellwood and Kafafy.

REFERENCES

Berggren, W. A. and Ouda, K., 2003, Upper Paleocene-lower Eocene planktonic foraminiferal biostratigraphy of the Dababiya section, Upper Nile Valley (Egypt): Micropaleontology, v. 49, supp 1, p. 61-92.

Berggren, W. A. and Ouda, K., 2003, Upper Paleocene-lower Eocene planktonic foraminiferal biostratigraphy of the Qreiya (Gebel Abu Had) section, Upper Nile Valley (Egypt): Micropaleontology, v. 49, supp 1, p. 105-122.

Dupuis, C., Aubry, M., Steurbaut, E., Berggren, W. A., Ouda, K., Magioncalda, R., Cramer, B. S., Kent, D. V., Speijer, R. P., and Heilmann-Clausen, C., 2003, The Dababiya Quarry Section: Lithostratigraphy, clay mineralogy, geochemistry and paleontology: Micropaleontology, v. 49, supp 1, p. 41-59.

Ellwood, B. B., Crick, R. E., Fernandez, J. L. G., Soto, F. M., Truyols-Massoni, M., El Hassani, A., and Kovas, E. J., 2001, Global correlation using magnetic susceptibility data from Lower Devonian rocks: Geology, v. 29, no. 7, p. 583-586.

Ellwood, B. B., Crick, R. E., El Hassani, A., Benoist, S. L., and Young, R. H., 2000, Magnetosusceptibility event and cyclostratigraphy method applied to marine rocks: Detrital input versus carbonate productivity: Geology, v. 28, no. 12, p. 1135-1138.

Kent, D. V. and Dupuis, C., 2003, Paleomagnetic study of the Paleocene-Eocene Tarawan Chalk and Esna Shale: Dual polarity remagnitizations of

Cenozoic sediments in the Nile Valley (Egypt): Micropaleontology, v. 49, supp 1, p. 139-146.

Knox, R. W. O'B., Aubry, M., Berggren, W. A., Dupuis, C., Ouda, K., Magioncalda, R., and Soliman, M., 2003, The Qreiya Section at Gebel Abu Had: Lithostratigraphy, clay mineralogy, geochemistry and biostratigraphy: Micropaleontology, v. 49, supp 1, p. 93-104.

Norris, R. D. and Röhl, U., 1999, Carbon cycling and chronology of climate warming during the Paleocene/Eocene transition: Nature, v. 401, p. 775-778.

Ouda, K., 2003, The Paleocene/Eocene boundary in Egypt: An overview: Micropaleontology, v. 49, supp 1, p. 15-40.

Ouda, K. and Berggren, W. A., 2003, Biostratigraphic correlation of the Upper Paleocene-Lower Eocene succession in the Upper Nile Valley: A synthesis: Micropaleontology, v. 49, supp 1, p. 179-212.

Röhl, U., Bralower, T. J., Norris, R. D., and Wefer, G., 2000, New Chronology for the late Paleocene thermal maximum and its environmental implications: Geology, v. 28, p. 927-930.

Soliman, M. F., 2003, Chemostratigraphy of the Paleocene/Eocene (P/E) boundary sediments at Gabal el-Qreiya, Nile Valley, Egypt: Micropaleontology, v. 49, supp 1, p. 123-138.

Wing, S. L., Bao, H., and Koch, P. L., 2000, An early Eocene cool period? Evidence for continental cooling during the warmest part of the Cenozoic: Warm climates in Earth history, eds. B. T. Huber et al., p. 197-236.

APPENDIX

In order to use magnetic susceptibility (MS) as a correlation tool, the basic principles of magnetism must be understood. Magnetic induction (B) is represented as a magnetic field associated with current flow in a straight wire ($B = 2I/kd$), where I = current, $k = N/amp^2$, and d = distance from the wire. Once this wire is bent into a loop, the magnetic induction is represented by $B = 2\pi I/kr$, where 2π accounts for the two dimensional character of the magnetic field. If this loop is repeated many times to form a solenoid, the magnetic induction is $4\pi nI/kl$, where n = number of turns and l = length of the solenoid. Finally, if the solenoid is bent into a loop creating a toroid, the magnetic induction is $4\pi\mu_r nI/k$ with μ_r = relative permeability of the center magnetic core. MS is derived from the relative permeability of a sample, where $\mu_r = 1 + \chi$ where χ is susceptibility. The relative permeability is related to the absolute permeability times the permeability of free space.

MS is a tensor of the second rank, having magnitude but no direction. This is physically represented by it's representation quadric, an ellipsoid, which is anisotropic because it has different properties in different directions (Nye, 1957). In most materials, MS is inherently anisotropic, with different values in various directions. When dealing with shales, the grains align themselves due to the natural stacking during deposition of elongate particles. This creates a parallel oriented anisotropy in shales and thus a magnetic foliation.

The MS was measured for whole rock shale sample pieces. Next, the samples were crushed and remeasured. The results are shown in figure A-1. The MS shows no statistical difference between whole and crushed shale pieces for 9

of these samples, and for one sample a statistically insignificant difference. This implies that physical orientation of the sample in the MS induction bridge used has essentially no effect on MS values and therefore the anisotropic character of the shales does not affect MS. All variation in values, with one exception, were within the range of standard deviation.